

Article

Study on the Grain Rotation of High-Purity Tantalum during Compression Deformation

Qianqian Zhu ^{1,2,3,*}, Yahui Liu ^{2,3,4}, Kexing Song ^{2,3,5,*}, Yanjun Zhou ^{1,2,3}, Xiaokang Yang ⁴, Shifeng Liu ⁶ 
and Lingfei Cao ⁶ 

¹ School of Materials Science and Engineering, Henan University of Science and Technology, Luoyang 471000, China; dazhou456@163.com

² Henan Key Laboratory of Non-Ferrous Materials Science & Processing Technology, Luoyang 471000, China; liuyh75@haust.edu.cn

³ Provincial and Ministerial Co-construction of Collaborative Innovation Center for Non-Ferrous Metal New Materials and Advanced Processing Technology, Luoyang 471000, China

⁴ School of Mechatronics Engineering, Henan University of Science and Technology, Luoyang 471000, China; yangxiaokang@haust.edu.cn

⁵ Henan Academy of Sciences, Zhengzhou 450002, China

⁶ College of Materials Science and Engineering, Chongqing University, Chongqing 400044, China; liusf06@cqu.edu.cn (S.L.); caolingfei@cqu.edu.cn (L.C.)

* Correspondence: zhuqianqian@haust.edu.cn (Q.Z.); kxsong@haust.edu.cn (K.S.)

Abstract: A compression experiment with electron backscatter diffraction (EBSD) measurements was designed to characterize the effect of the microtexture on the grain rotation process. The rotation degrees of more than 180 grains before and after the compression were calculated. Results showed that grains with different crystallographic orientations experienced various rotation degrees. Furthermore, grains in certain microtexture regions also had varying degrees of rotation. The compression led to the lattice rotation and change in orientation of individual grains, but the relative misorientation between grains has not changed much in the microtexture region. The microtexture region, as a whole, participated in the compression process. The similar slipping behavior of the grains in the region promoted the slip transmission between the neighboring grains. Thus, the amount of piled-up dislocations at grain boundaries inside the microtexture region are less than that at grain boundaries outside the microtexture region, leading to a small stored energy density for grain boundaries inside the microtexture region.

Keywords: Tantalum; grain subdivision; strain localization; crystallographic rotation



Citation: Zhu, Q.; Liu, Y.; Song, K.; Zhou, Y.; Yang, X.; Liu, S.; Cao, L. Study on the Grain Rotation of High-Purity Tantalum during Compression Deformation. *Crystals* **2022**, *12*, 676. <https://doi.org/10.3390/cryst12050676>

Academic Editor: Sławomir Grabowski

Received: 12 April 2022

Accepted: 4 May 2022

Published: 9 May 2022

Publisher's Note: MDPI stays neutral with regard to jurisdictional claims in published maps and institutional affiliations.



Copyright: © 2022 by the authors. Licensee MDPI, Basel, Switzerland. This article is an open access article distributed under the terms and conditions of the Creative Commons Attribution (CC BY) license (<https://creativecommons.org/licenses/by/4.0/>).

1. Introduction

Research on microstructures optimization has become one of the forward positions of Tantalum (Ta) and its alloys because of their application in integrated circuit (IC) chips [1,2]. Specifically, the Ta sheet served as sputtering target material in the circuit deposition process, during which atoms in differently oriented planes in the target were deposited to the IC chips. Since the density of atoms is different in planes with different crystallographic orientations, the sputtering rates for these planes are pretty different, which would lead to various thicknesses of films upon the deposition process and then would significantly affect the stability of the circuit [3,4]. From this point of view, randomizing the orientation distribution is key to improving the sputtering performance. Generally, severe plastic deformation would be helpful for randomizing orientation distribution, as reported in many laboratory investigations. However, in conventional deformation processes such as rolling, extension, or compression, grains in the sheet underwent various subdivisions and rotation processes, leading to diverse microstructures and textures [5,6]. Thus, understanding the deformation mechanism may help to control the microstructure and randomize the orientation distribution.

The deformation is realized by the activation of slip systems in grains, and the activation is mainly related to the angle between stress direction and the crystal plane orientation [7]. Thus, the microtexture, the preferential orientation distribution in local regions, would influence the activation process and lead to a complicated situation of flow stress [8,9]. Grains rotate to some extent because of the limitation of grain boundaries during deformation, and this rotation behavior should be similar for grains with similar crystallographic orientations. There would be significant differences in the subdivision and rotation behavior between the regions with strong texture and random orientations [10,11]. Although orientation distribution in local regions would significantly affect the microstructure evolution and sputtering performance of the Ta sheet, few studies have focused on detailed characterization to investigate such a deformation process.

In the present study, using the quasi-in situ electron backscatter diffraction (EBSD) technique, we investigated the grain rotation behavior of a high-purity polycrystalline Ta sheet, including rotation degree, strain localization, and the evolution of microtexture during deformation. EBSD technique has advantages of high spatial resolution and high speed for crystallographic information collection in polycrystalline aggregates, considered as a very conducive tool for investigating grain rotations and stress concentration in local regions upon the plastic deformation [12,13]. Generally, EBSD can track the lattice rotation of individual grains by reconstructing the orientation distribution of multiple grains under different deformation degrees. A study on this topic would significantly advance the deformation mechanism knowledge of body-centered cubic (BCC) metal at a crystallographic level and greatly deepen the understanding of the texture evolution of the sputtering target in an intuitive way.

2. Materials and Methods

The initial Ta (99.95 wt%, Ningxia Orient Tantalum Industry Co. Ltd., Shizuishan, China) sheet was annealed at 1250 °C for 2 h in a vacuum environment to obtain a fully recrystallized microstructure before the compression [14]. The chemical composition is shown in Table 1. A block of annealed Ta specimen with size of 10(RD) × 9(TD) × 7(ND) mm³ was compressed along the ND direction to achieve a reduction of 6.48% using a Shimadzuag-X10KM test machine with a strain rate of 10^{−3} s^{−1}.

Table 1. Chemical composition of high purity Ta (wt. ppm).

C	N	H	O	Nb	Mo	W	Ti	Si	Fe	Ni	Ta
9	20	2	30	6.4	0.14	0.61	<0.001	<0.005	<0.005	<0.005	Balance

The surface of the specimen for characterization was in the center of rolling direction–normal direction (RD–ND) plane. Before compression, the surface was electrolytically polished with a mixture of hydrofluoric acid and sulfuric acid (1:9 by volume) at ambient temperature. The microstructure and microtexture of a designed area, marked by microhardness indents, were characterized by EBSD, which served as the initial microstructure and microtexture. After compression, the surface was slightly polished using alcohol. The same area was characterized by EBSD to record the changes in microstructure and microtexture so that the rotations of individual grains could be tracked during compression, which was otherwise very difficult to be realized by conventional experimental methods (as shown in Figure 1). In addition, secondary electron (SE) images were also taken within the marked areas before and after the compression deformation.

The EBSD measurement was carried out using a JEOL JSM-7800F scanning electron microscope (SEM) with an accelerating voltage of 20 kV. The EBSD data were then analyzed by Channel 5 software equipped in an Aztec EBSD system (Oxford Instruments), and the data were cleaned up for one time with three grades (the full grade is eight). The area used in the EBSD analysis contained more than 180 grains, and the grains were defined with a misorientation tolerance of 10° and a minimum grain size of 5 pixels.

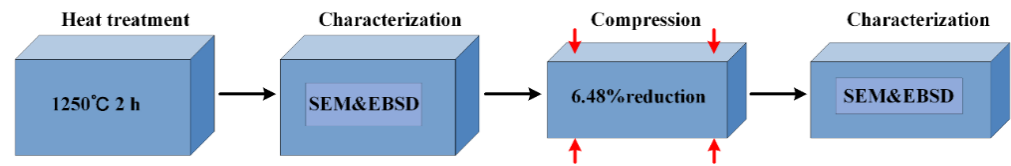


Figure 1. Processing and characterization schedule.

3. Results

Figure 2a and b show the microstructures of the specimen before and after the compression deformation, respectively. The surface of the specimen is very smooth before compression (Figure 2a), while most of the grains have a clear outline, bulging or sagging, after the compression (Figure 2b). In addition, a certain degree of ups and downs is observed on sample surface in the micro-view due to serious deformation of some certain grains.

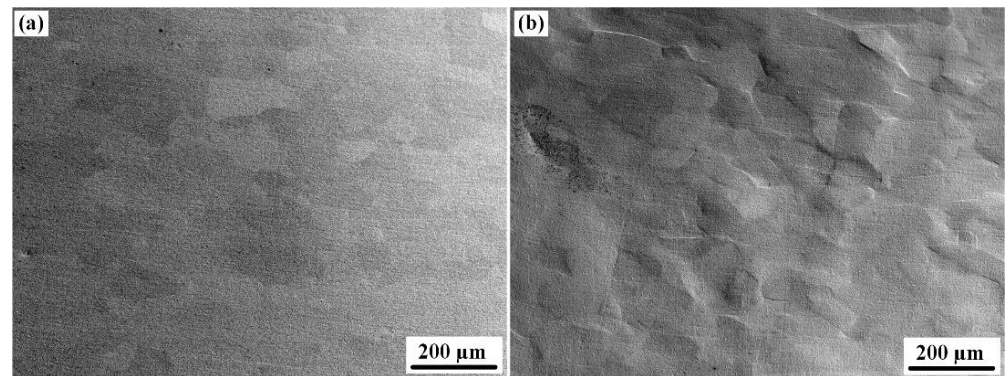


Figure 2. The tracking SE micrographs of the specimen. (a) microstructure before compression, (b) microstructure of the same area after compression.

The tracking EBSD characterization is shown in Figure 3 (1204 points \times 903 points, step size 1 μm). The scanned area consists of about 180 grains on the RD–ND section at the center region (Figure 3a). The grains are a little elongated along the RD direction and with an average size of about 42 μm . After a 6.48% thickness reduction, all these grains can still be identified, and the orientation change of each grain can be noticed from the variations in color within the individual grains (Figure 3b).

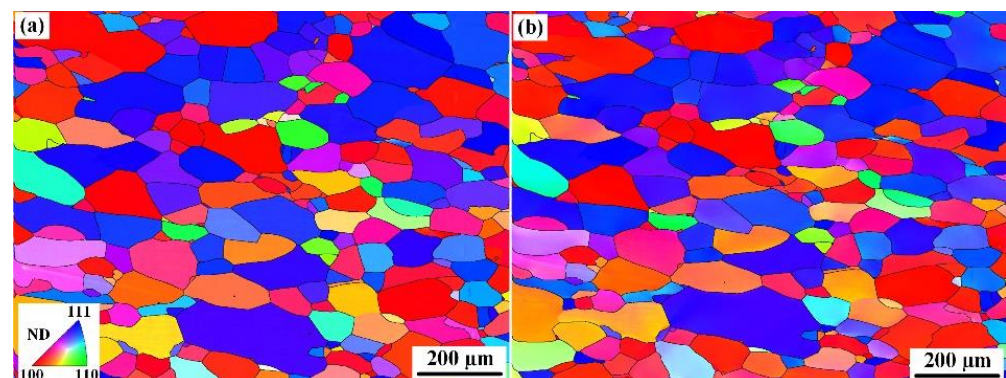


Figure 3. The tracking orientation imaging maps (OIMs) of the specimen before and after deformation. (a) OIM before deformation, (b) OIM of the same area after deformation.

It should be mentioned that many indentation marks were made on the testing surface of the specimen to make sure that the testing area after compression is the same one as that before compression. In addition, to minimize the crystallographic orientation error

introduced by the specimen alignment operation, very careful position correction work was carried out during the measurement of EBSD. Results showed that the SEM micrographs (Figure 2) and OIMs (Figure 3) from EBSD before and after the compression are in good agreement in the present study.

The initial texture plays a crucial role in the deformation process, and the texture evolution is of great importance for understanding the deformation mechanism. Thus, the microtexture of the specimen before and after the compression was analyzed in a quantitative way to investigate the texture evolution mechanism during compression process. As shown in the pole figure (PF) of the specimen before compression, the maximal orientation density is 6.40 (Figure 4a), which means the distribution of orientations is not random in the initial stage. After compression, the maximal orientation density increases to 6.76, as shown in Figure 3b. In particular, the volume fraction of $\{111\}\langle uvw\rangle\langle 111\rangle//ND$ grains increases from 34.7% to 36.5%, while the volume fraction of $\{100\}\langle uvw\rangle\langle 100\rangle//CD$ grains increases from 25.5% to 26.7% after compression.

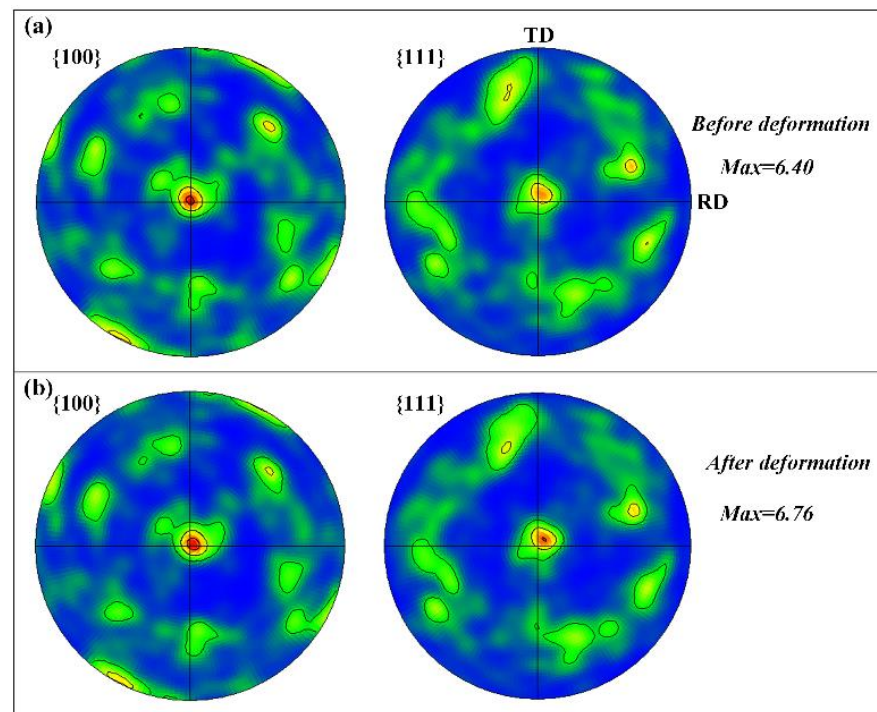


Figure 4. Pole figures (PFs) of the specimen (a) before compression and (b) after compression.

During plastic deformation, the shape and textures of the polycrystalline metals change via grain rotation and subdivision. At the grain level, the shape and crystallographic orientation of each grain changed because of the lattice rotation. The orientation changes in each grain lead to the microtexture evolution upon the deformation process [10,15,16]. Thus, it is necessary to investigate the lattice rotation process in order to establish the relationship between the microtexture and the deformation parameters.

Figure 5 shows the crystallographic orientation rotation degree of grains caused by compression. In particular, more than 180 grains were characterized in the scanning area, the Euler angles for grains before and after deformation were recorded, one by one, and then their rotation degree was calculated and labeled on the figure, respectively. It is found that grains with different crystallographic orientations have various rotation degrees. However, some grains with similar orientations show significant differences in their rotation degrees.

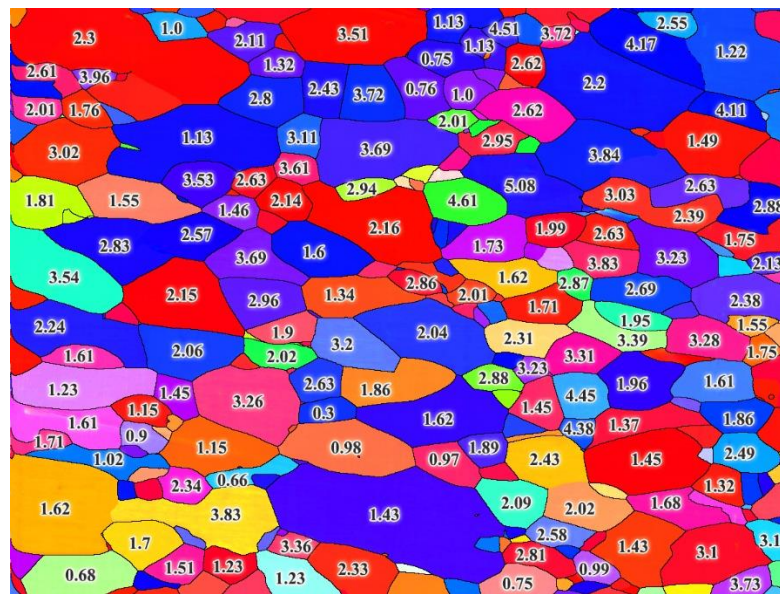


Figure 5. The orientation rotation degrees for grains caused by compression.

4. Discussion

During plastic deformation, the external force produces dislocations in the crystallographic lattice. The movement of dislocations depends on the activation of slip systems, causing the two sides of the planes to slide with respect to each other [16,17]. The change in microstructures is the result of thousands of such processes. In addition, during these processes, the dynamic of the grains is coupled to ensure the adjoin and stress equilibrium between grain boundaries of the adjacent grains. Furthermore, the crystallographic orientations must rotate with respect to each other to facilitate such processes because of the limitation of grain boundaries.

Grain subdivision and rotation are related to the activation of slip systems. The slip activation depends on the relationship between stress direction and slip systems, the angle between stress direction and slip plane, and the angle between stress direction and slip direction [17,18]. It means that the grain rotation depends upon its crystallographic orientation. From this point of view, grains with similar orientations should rotate with similar degrees upon deformation since their relationships with stress direction are identical to each other. As shown in Figure 5, grains with different orientations did exhibit variable rotation degrees, and the interesting point is that some grains with similar orientations show highly differentiated rotation degrees. To investigate this point in detail, some of these grains were extracted from the EBSD data and then reconstructed in Figure 5.

Figure 6 shows several grains with {111} orientations (in blue), exhibiting a strong micro-texture in the local region, however they have various rotation degrees (Figure 5). The further calculation revealed that the average rotation degree of these grains is 2.163° , while the average value for the other grains is 2.435° after compression. Here raises a question: how did the micro-texture influence the grain rotation process, or how did the grains inside and outside the orientation concentrated region subdivide upon deformation? To answer this question, boundaries inside and outside the region were numbered, respectively, as shown in Figure 6. The misorientations of adjacent grains were calculated. The deviations (or misorientations) of the misorientations before and after deformation was further calculated and linked into a line, as shown in Figure 7.

As shown in Figure 7, large deviation degrees of misorientation appeared in grain boundaries outside the micro-texture region (External GBs), and their average value of the misorientation reached 1.4° after deformation. While for grain boundaries inside the micro-texture region (Internal GBs), their average value of misorientation is much lower, about 1° after deformation, and the volatility of deviation degrees is smaller than that of

outside ones. It means that grains outside the micro-texture region experienced a larger deformation upon compression. From this point of view, the micro-texture region, as a whole, participates in the subdivision and rotation processes during deformation.

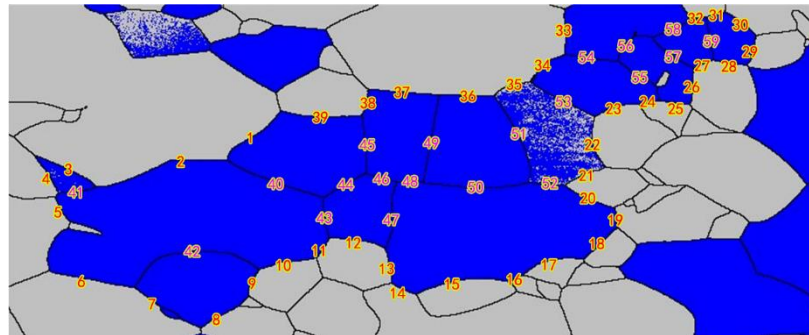


Figure 6. Some grains extracted from EBSD data in Figure 5.

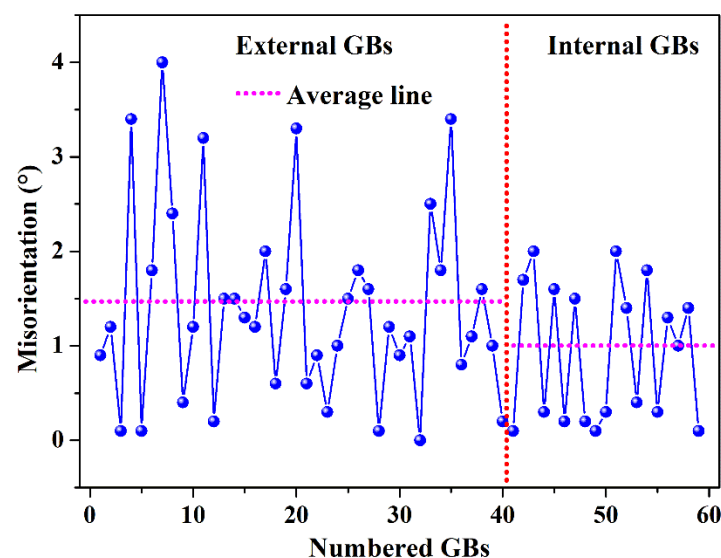


Figure 7. The differences in the misorientations before and after deformation.

In the previous studies, γ -fiber texture, which mainly consists of $\{111\}\langle uvw \rangle$ orientations, was found to undergo inhomogeneous deformation and begat various kinds of dislocation structures such as deformation bands, microbands, or microshear bands [14,19,20]. These dislocations would evolve into coarse grains during heat treatment, leading to the formation of new strong textures in the annealed sheets [21]. The occurrence of different dislocation configurations, in essence, is caused by the maintenance of primary slipping upon deformation [22]. The appearance of primary slipping aims to coordinate the strong stress concentration in the local region [19]. From this point of view, a strong texture, as illustrated in this study, always causes stress concentration in local regions.

Grain–grain interaction effects may manifest themselves by local changes in microstructure and crystallography in the grain boundary region during deformation [15,23]. Grain boundaries often hinder the transmission of dislocations and lead to the dislocation pile-up, thus the material becomes harder to deform. It means that the deformation degree is larger in grain boundary regions than that in internal regions of grains. From this point of view, the density of pile-up dislocations at grain boundaries outside the micro-texture region is larger than that of grain boundaries inside the micro-texture region.

Most of the work is released as heat during plastic deformation, and only a very small amount ($\sim 1\%$) remains as energy stored in the material. Almost all stored energy is derived from the accumulation of dislocations formed by the activation of slip systems

in grains [24]. As aforementioned, the density of pile-up dislocations is higher for grain boundaries outside the micro-texture region, thus the stored energy is larger in these boundaries. We quantitatively evaluated the stored energy for boundaries outside and inside the micro-texture region, respectively, using the band contrast (BC) values collected from EBSD data [25]. More precisely, the BC value of EBSD data can reflect the extent to which the different regions deformed in a testing area by detecting the grey levels corresponding to the maximum and the minimum in the Hough transform [26,27].

To investigate the stored energy of different grain boundaries quantitatively, the testing region in Figure 6 was subdivided into 48 blocks (both horizontal and vertical directions), respectively, as shown in Figure 8a and b. The stored energy for a block 'i', S_i , is proportional to the pattern quality index, H_i , which can be calculated in the following relation [28]:

$$S_i \propto H_i = 10 \left[1 - \frac{Q_i(g_i) - Q_{min}}{Q_{max} - Q_{min}} \right]$$

in which $Q_i(g_i)$ is the pattern quality for block 'i', and Q_{min} and Q_{max} are the minimum and maximum pattern quality of the aggregate, respectively, which can be directly collected from the Tango in Channel 5 software. In addition, the pattern quality index has a spectrum from 5 to 10 after being normalized by the equation. Then energy values for all blocks were evaluated and connected into lines, as shown in Figure 8c.

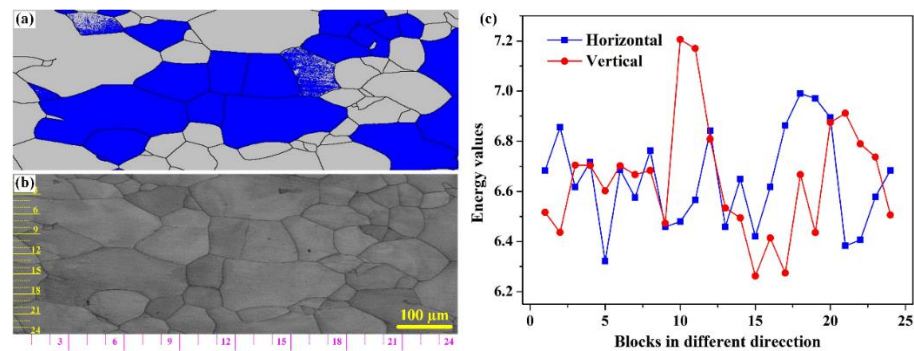


Figure 8. Values of stored energy for different blocks in the testing area. The extracted grains (a) and the BC map (b), and the evaluated stored energy values (c).

The stored energy values fluctuate significantly through the vertical direction of the testing area, while those fluctuate moderately through the horizontal direction. Especially blocks of 10 and 11 in the vertical direction and blocks of 16 and 17 in the horizontal direction contain large stored energy in the testing area. Further analysis conclusively shows that these blocks contain quite a few grain boundaries outside the micro-texture region. In contrast, blocks of 15 and 17 in the vertical direction, and blocks of 21 and 22 in the horizontal direction, with many grain boundaries inside the micro-texture region, are of low stored energy values.

From the stored energy calculation, we know that the density of pile-up dislocations is higher in grain boundaries outside the microtexture region, leading to strain localization in regions near the boundaries. Dislocations source and pile-up are always expected to exist at grain boundaries, and the deformation is believed to be proceeding mostly by the grain boundaries via a particular accommodation mechanism [15]. The transmission of dislocations between grains is mainly related to the activation of slip systems, the deformation coordination, and the stress concentration at grain boundaries [29]. Here, deformation coordination reflects the relationship between the slip systems activated in the adjacent grains, depending on the angle between their slip planes, and the angle between their slip directions. In general, the transmission is easy for dislocations when the adjacent grains have similar crystalline orientations. Thus, the density and the stored energy for boundaries inside the micro-texture region are lower than those outside the micro-texture region.

Comparing Figure 5 with Figure 7, we can find that there is little difference in the crystallographic rotation degrees of the grains inside and outside the micro-texture region, which means the subdivision or deformation degree is similar for grains both inside and outside the micro-texture region. However, the stored energy calculated from BC values is indeed larger for grain boundaries outside the micro-texture region than those inside the micro-texture region. Here raises a question: What leads to such a contradiction or conflict? For grains with similar crystallographic orientations, that is, the micro-texture region, their deformation behavior is similar due to the activation of similar slip systems. The deformation leads to the lattice rotation and orientation change in individual grains, but the relative misorientation between grains has not changed much in the micro-texture region during deformation. The micro-texture region, as a whole, participated in deformation process. In addition, the similar slipping behavior of grains in the region promoted the slip transmission between the neighboring grains. Thus, the piled-up dislocations for the boundaries inside the micro-texture region are small, leading to a low stored energy density. Similar situations were also found in the previous investigations, the θ -fiber texture, which mainly consists of $\{100\}\langle uvw \rangle$ orientations, subdivided with multiple slipping upon deformation [14]. The boundaries in the texture underwent a moderate deformation, while the boundaries near the $\{111\}$ grains subdivided into many kinds of substructures. In addition, these substructures with large sizes served as nucleuses upon annealing and stimulated the formation fine grains with random orientations.

Similar situations were also found in the previous investigations, in essence, this is a kind of intergranular deformation [18]. The intergranular deformation mainly involves the influence of grain boundaries on stress flow in a local region. The θ -fiber texture, which mainly consists of $\{100\}\langle uvw \rangle$ orientations, always exhibits homogeneous deformation [22]. The homogeneous deformation is mainly contributed to the multiple slipping in $\{100\}$ grains, in which the split and twist degrees are not very large for the boundaries, while the boundaries in γ -fiber texture always split into very small substructures and have distinct orientation gradients [30]. However, on the other hand, such kind of grain subdivision and orientation rearrangement introduced by strong shear in local regions would evolve into fine grains and randomly distributed orientations during the subsequent heat treatment.

5. Conclusions

This study investigates the lattice rotation behavior of grains in a high-purity Ta sheet upon compression. EBSD technology was employed to characterize the microstructure and local orientations within the same area on the surface of the specimen during compression process. The following conclusions were drawn:

- (1) The initial texture is strong before compression, and then the volume fraction of $\{111\}\langle uvw \rangle$ orientations increases from 34.7% to 36.5%, while the volume fraction of $\{100\}\langle uvw \rangle$ orientations increases from 25.5% to 26.7% after compression;
- (2) The rotation degrees are different for grains with different crystallographic orientations because of the activation of slip systems. But at the same time, experimental results show that some grains with similar orientations possessed highly differentiated rotation degrees;
- (3) The deviation degrees of misorientations for the adjacent grains before and after deformation was further analyzed, and the results show that the average deviation degree is more significant in outside boundaries than that of inside boundaries of the microtexture region, which means the deformation degree is more serious for outside boundaries;
- (4) The density of pile-up dislocations is larger in grain boundaries outside the micro-texture region than the inside ones due to the fact that the transmission is easy for dislocations in the micro-texture region since the adjacent grains have similar crystallographic orientations.

Author Contributions: Conceptualization, Q.Z. and Y.L.; investigation, Q.Z., Y.L. and X.Y.; data curation, Q.Z. and Y.L.; writing—original draft preparation, Q.Z. and Y.L.; writing—review and editing, S.L., Y.Z. and L.C.; supervision, K.S.; funding acquisition, Q.Z., Y.L., X.Y. and S.L. All authors have read and agreed to the published version of the manuscript.

Funding: This research was funded by the National Key R&D Program of China (2021YFB3400800), Key R&D and promotion projects in Henan Province (Grants 222102230046, 212102210279), Postdoctoral research fellowship at Henan University of Science and Technology (4002-13554027), China Engineering Science and technology development strategy Henan Research Institute strategic consulting research project (2021HENZDA02), Zhongyuan scholar workstation funded project (214400510028).

Data Availability Statement: The processed data required to reproduce these findings cannot be shared at this time as the data also forms part of an ongoing study.

Acknowledgments: We thank Chao Deng for the high-quality microstructure characterization of tantalum in Electron Microscopy Center of Chongqing University.

Conflicts of Interest: No conflict of interest exists in the submission of this manuscript, and all authors approve the manuscript for publication. The work described was original research that has not been published previously and is not under consideration for publication elsewhere, in whole or in part. All the authors listed have approved the manuscript that is enclosed.

References

1. Jason, M.D.; Mojib, S.; Debapriya, P.M.; Anirudh, U.; Tatsuya, S.; Srinivasan, C. Cutting of tantalum: Why it is so difficult and what can be done about it. *Int. J. Mach. Tool. Manu.* **2020**, *157*, 103607.
2. Alexander, T. Effect of Moisture on AC Characteristics of Chip Polymer Tantalum Capacitors. *IEEE T. Comp. Pack. Man.* **2019**, *9*, 2282–2289.
3. Michaluk, C.A. Correlating Discrete Orientation and Grain Size to the sputter deposition properties of tantalum. *J. Electron. Mater.* **2002**, *31*, 2–9. [[CrossRef](#)]
4. Zhang, Z.; Kho, L.; Wickersham, C.E. Effect of grain orientation on tantalum magnetron sputtering yield. *J. Vac. Sci. Technol.* **2006**, *24*, 1107–1111. [[CrossRef](#)]
5. Roberto, B.F.; Terence, G.L. Processing Magnesium and Its Alloys by High-Pressure Torsion: An Overview. *Adv. Eng. Mater.* **2018**, *21*, 1801039.
6. Hagihara, K.; Okamoto, T.; Yamasaki, M.; Kawamura, Y.; Nakano, T. Electron backscatter diffraction pattern analysis of the deformation band formed in the Mg-based long-period stacking ordered phase. *Scr. Mater.* **2016**, *117*, 32–36. [[CrossRef](#)]
7. Bridier, F.; Villechaise, P.; Mendez, J. Analysis of the different slip systems activated by tension in a α/β titanium alloy in relation with local crystallographic orientation. *Acta Mater.* **2005**, *53*, 555–567. [[CrossRef](#)]
8. Chen, L.; Chen, G.J.; Tang, J.W.; Zhao, G.Q.; Zhang, C.S. Evolution of grain structure, micro-texture and second phase during porthole die extrusion of Al–Zn–Mg alloy. *Mater. Charact.* **2019**, *158*, 109953. [[CrossRef](#)]
9. Dini, G.; Ueji, R.; Najafizadeh, A.; Monir-Vaghefi, S.M. Flow stress analysis of TWIP steel via the XRD measurement of dislocation density. *Mat. Sci. Eng. A* **2010**, *527*, 2759–2763. [[CrossRef](#)]
10. Poulsen, H.F.; Margulies, L.; Schmidt, S.; Winther, G. Lattice rotations of individual bulk grains. *Acta Mater.* **2003**, *51*, 3821–3830. [[CrossRef](#)]
11. Winther, G.; Margulies, L.; Schmidt, S.; Poulsen, H.F. Lattice rotations of individual bulk grains Part II: Correlation with initial orientation and model comparison. *Acta Mater.* **2004**, *52*, 2863–2872. [[CrossRef](#)]
12. Wilkinson, A.J.; Britton, T.B. Strains, planes, and EBSD in materials science. *Mater. Today* **2012**, *15*, 366–376. [[CrossRef](#)]
13. Íris, C.; Sónia, S. Recent Advances in EBSD Characterization of Metals. *Metal* **2020**, *10*, 1097.
14. Liu, Y.H.; Liu, S.F.; Lin, N.; Zhu, J.L.; Deng, C.; Liu, Q. Effect of strain path change on the through-thickness microstructure during tantalum rolling. *Int. J. Refract. Met. Hard Mater.* **2020**, *87*, 105168. [[CrossRef](#)]
15. Lin, X.; Chen, Z.Y.; Shao, J.B.; Xiong, J.Y.; Hu, Z.; Liu, C.M. Deformation mechanism, orientation evolution and mechanical properties of annealed cross-rolled Mg–Zn–Zr–Y–Gd sheet during tension. *J. Magnes. Alloy* **2021**. [[CrossRef](#)]
16. Margulies, L.; Winther, G.; Poulsen, H.F. In Situ Measurement of Grain Rotation During Deformation of Polycrystals. *Science* **2001**, *291*, 2392–2394. [[CrossRef](#)]
17. Gallé, C.; Robertson, I.M.; He, B.C.M.-R. Dislocation Grain Boundary Interactions in Irradiated Metals. *EPJ Web Conf.* **2016**, *115*, 04001.
18. Sun, J.; Jin, L.; Dong, J.; Wang, F.; Dong, S.; Ding, W.; Luo, A.A. Towards high ductility in magnesium alloys—The role of intergranular deformation. *Int. J. Plast.* **2019**, *123*, 121–132. [[CrossRef](#)]
19. Zhu, L.; Marc, S.; Bert, V. Deformation banding in a Nb polycrystal deformed by successive compression tests. *Acta Mater.* **2012**, *60*, 4349–4358. [[CrossRef](#)]
20. Liu, Y.H.; Liu, S.F.; Deng, C.; Fan, H.Y.; Yuan, X.L.; Liu, Q. Inhomogeneous deformation of $\{111\}\langle uvw \rangle$ grain in cold rolled tantalum. *J. Mater. Sci. Technol.* **2018**, *34*, 2178–2182. [[CrossRef](#)]

21. Zhang, Z.Q.; Chen, D.D.; Zhao, H.; Liu, S.F. A comparative study of clock rolling and unidirectional rolling on deformation/recrystallization microstructure and texture of high purity tantalum plates. *Int. J. Refract. Met. Hard Mater.* **2013**, *41*, 453–460. [[CrossRef](#)]
22. Liu, Y.H.; Liu, S.F.; Zhu, J.L.; Deng, C.; Fan, H.Y.; Cao, L.F.; Liu, Q. Strain path dependence of microstructure and annealing behavior in high purity tantalum. *Mater. Sci. Eng. A* **2017**, *707*, 518–530. [[CrossRef](#)]
23. Kondo, S.; Mitsuma, T.; Shibata, N.; Ikuhara, Y. Direct observation of individual dislocation interaction processes with grain boundaries. *Sci. Adv.* **2016**, *2*, e1501926. [[CrossRef](#)] [[PubMed](#)]
24. Lu, X.; Fionn, P.E.D.; Xu, Y.L. A crystal plasticity investigation of slip system interaction, GND density and stored energy in non-proportional fatigue in Nickel-based superalloy. *Int. J. Fatigue* **2020**, *139*, 105782. [[CrossRef](#)]
25. Deng, C.; Liu, S.F.; Fan, H.Y.; Hao, X.B.; Ji, J.L.; Zhang, Z.Q.; Liu, Q. Elimination of Elongated Bands by Clock Rolling in High-Purity Tantalum. *Metall. Mater. Trans. A* **2015**, *46*, 5477–5481. [[CrossRef](#)]
26. Wilkinson, A.J.; Dingley, D.J. Quantitative deformation studies using electron back scatter patterns. *Acta Metall. Mater.* **1991**, *39*, 3047–3055. [[CrossRef](#)]
27. Oyarzábal, M.; Martínez-de-Guerenu, A.; Gutiérrez, I. Effect of stored energy and recovery on the overall recrystallization kinetics of a cold rolled low carbon steel. *Mat. Sci. Eng. A* **2008**, *485*, 200–209. [[CrossRef](#)]
28. Choi, S.-H.; Jin, Y.-S. Evaluation of stored energy in cold-rolled steels from EBSD data. *Mat. Sci. Eng. A* **2004**, *371*, 149–159. [[CrossRef](#)]
29. Bieler, T.R.; Eisenlohr, P.; Zhang, C.; Phukan, H.J.; Crimp, M.A. Grain boundaries and interfaces in slip transfer. *Curr. Opin. Solid State Mater. Sci.* **2014**, *18*, 212–226. [[CrossRef](#)]
30. Liu, Y.H.; Liu, S.F.; Fan, H.Y.; Deng, C.; Cao, L.F.; Ni, H.T.; Liu, Q. Orientation-dependent grain boundary characteristics in tantalum upon the change of strain path. *Mater. Character.* **2019**, *154*, 277–284. [[CrossRef](#)]